

Novel aluminium phenyl, benzyl, and bromobenzylphosphonates: structural characterisation and hydration–dehydration reactions†

Gérald Chaplais, Jean Le Bideau,* Dominique Leclercq, Hubert Mutin and André Vioux

Laboratoire de Chimie Moléculaire et Organisation du Solide UMR CNRS 5637, Université Montpellier II - cc 007, Place Eugène Bataillon, F-34095 Montpellier cedex 5, France.
E-mail: lebideau@crit1.univ-montp2.fr; Fax: 33 467 143 852; Tel: 33 467 143 853

Received 6th January 2000, Accepted 17th April 2000

Published on the Web 30th May 2000

Reaction of phosphonic acids $\text{RPO}(\text{OH})_2$ (R = phenyl, benzyl, 4-bromobenzyl) with aluminium nitrate and sulfate under various hydrothermal conditions led to three novel aluminium phosphonates, $\text{Al}(\text{OH})(\text{O}_3\text{PCH}_2\text{C}_6\text{H}_4\text{Br})\cdot\text{H}_2\text{O}$, $\text{Al}(\text{OH})(\text{O}_3\text{PCH}_2\text{C}_6\text{H}_5)\cdot\text{H}_2\text{O}$ and $\text{Al}_2(\text{O}_3\text{PC}_6\text{H}_5)_3\cdot\text{H}_2\text{O}$. All the compounds were characterised by powder XRD, elemental analysis, TGA, ^{27}Al and ^{31}P MAS NMR and IR spectroscopy. The same tools were used to study the dehydration–rehydration reactions. Refinement of the structure of $\text{Al}(\text{OH})(\text{O}_3\text{PCH}_2\text{C}_6\text{H}_4\text{Br})\cdot\text{H}_2\text{O}$ by the Rietveld method showed a lamellar arrangement similar to the methyl analogue $\zeta\text{-Al}(\text{OH})(\text{O}_3\text{PCH}_3)\cdot\text{H}_2\text{O}$. $\text{Al}(\text{OH})(\text{O}_3\text{PCH}_2\text{C}_6\text{H}_4\text{Br})\cdot\text{H}_2\text{O}$ crystallises in the monoclinic system, space group $P2_1/c$ with unit cell parameters $a = 16.4972(2)$ Å, $b = 7.0673(1)$ Å, $c = 9.4950(2)$ Å and $\beta = 113.477(1)^\circ$. Based on the powder XRD, IR and NMR data the two benzyl compounds were found to be isostructural.

Introduction

Hybrid organic–inorganic materials represent an extensive class of compounds, within which metal phosphonates possess a special place as they can be obtained with most metals and offer a wide range of structures. As a result they are used for the structural and physical design of new materials. Indeed, metal phosphonates have been studied as ion exchangers, sorbents, sensors, proton conductors, non-linear optical materials and catalysts, as well as magnetic models.¹ Metal phosphonates have been described with a wide range of organic substituents and divalent, trivalent and tetravalent metal atoms.¹ To date the chemistry of trivalent metal phosphonates includes iron,² bismuth,³ lanthanum,⁴ samarium and cerium,⁵ praseodymium, neodymium, and gadolinium,⁶ and the Group 13 elements indium,⁷ gallium⁸ and aluminium.

The last compounds have been preceded by aluminophosphates, which are attractive materials due to some members of their family which offer zeolitic type microporosity. The use of templates or structure-directing agents allows us to obtain a wide variety of structures, ranging from molecular entities⁹ up to opened three-dimensional networks.^{10,11} However, the chemical features of the walls in porous aluminophosphates are a limiting factor for their applications. Alternatively, phosphonate units can simultaneously introduce steric and chemical constraints which can direct the framework and determine the surface properties of the material.

The rich structural and compositional diversity of aluminium phosphonates results from the many ways of combining the four-, five- or six-coordinated aluminium cation with anionic phosphonate tetrahedra, $[\text{RPO}_3]^{2-}$ and $[\text{RP}(\text{OH})\text{O}_2]^-$. Phases with the composition $\text{Al}/\text{P} = 2/3$, obtained using $[\text{RPO}_3]^{2-}$ tetrahedra, do not involve any OH groups. Therefore aluminium phosphonate may be classified into acidic phases (POH groups present) or basic phases (AlOH groups present) depending on whether the Al/P ratio is higher or lower than 2/3. Taking into account the H_2O content, a triangular diagram gives a suitable representation of the composition range of

these compounds, as illustrated for the aluminium phenylphosphonates in Fig. 1. In this representation the lines bounding the H_2O apex to the various Al/P compositions describe the related hydration–dehydration reactions. It is noteworthy that these reactions play a determining role in the thermal stability of these compounds for materials applications. So, for a given composition (one point of the diagram), it is important to determine which phases actually exist, and which intermediates form during the course of their hydration–dehydration reactions in relation to their structure.

The literature reflects the diversity of the framework dimensionalities obtainable for aluminium phosphonates. Besides the molecular aluminium phosphonate cages,¹² two reported aluminium methylphosphonate structures are open three-dimensional frameworks,^{13,14} and two are lamellar.^{15–17} One lamellar aluminium carboxymethylphosphonate has also been reported.¹⁸ Recently, six aluminium phenylphosphonates have been identified,¹⁹ including $\text{Al}_2(\text{O}_3\text{PC}_6\text{H}_5)_3\cdot 2\text{H}_2\text{O}$, $\text{Al}_2(\text{O}_3\text{PC}_6\text{H}_5)_3$, $\text{Al}(\text{OH})(\text{O}_3\text{PC}_6\text{H}_5)$ and $\alpha\text{-Al}(\text{HO}_3\text{PC}_6\text{H}_5)(\text{O}_3\text{PC}_6\text{H}_5)\cdot\text{H}_2\text{O}$. However the crystal-

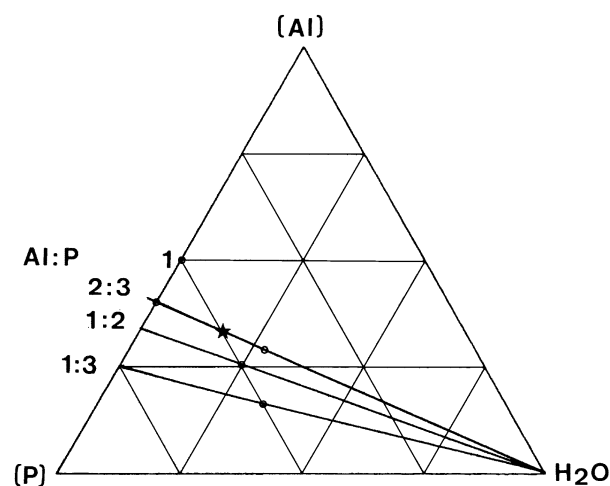


Fig. 1 Aluminium phenylphosphonates ternary diagram (molar ratios). The circles and the star denote compounds from ref. 18 and from the present work, respectively.

†Electronic supplementary information (ESI) available: X-ray powder diffraction data and Rietveld plots. See <http://www.rsc.org/suppdata/jm/b0/b0001031/>

lographic structure has been determined only for the latter phosphonate, showing a lamellar arrangement.

In the present work, we report the synthesis and characterisation of three novel aluminium phosphonates: one bromobenzyl derivative $\text{Al}(\text{OH})(\text{O}_3\text{PCH}_2\text{C}_6\text{H}_4\text{Br})\cdot\text{H}_2\text{O}$ the structure of which is reported, one benzyl derivative $\text{Al}(\text{O}-\text{H})(\text{O}_3\text{PCH}_2\text{C}_6\text{H}_5)\cdot\text{H}_2\text{O}$ and one phenyl derivative $\text{Al}_2(\text{O}_3\text{PC}_6\text{H}_5)_3\cdot\text{H}_2\text{O}$. They have been characterised by PXRD, TGA, ^{27}Al and ^{31}P MAS NMR and IR spectroscopy. Dehydration–rehydration reactions have been studied for each compound.

Experimental

Synthesis

Aluminium nitrate nonahydrate, aluminium sulfate octadecahydrate 98% and triethyl phosphite 98% were purchased from Aldrich. Phenylphosphonic acid 98%, benzylbromide 98%, 4-bromobenzylbromide 98% and bromotrimethylsilane 98% were purchased from Acros. Before use, the phenylphosphonic acid was recrystallised in acetonitrile. Benzyl and 4-bromobenzylphosphonic acids were prepared by silylation and hydrolysis of their respective phosphonate diethyl ester.²⁰ The esters were synthesized from benzylbromide and 4-bromobenzylbromide by the Arbuzov reaction with triethyl phosphite.²¹

$\text{C}_6\text{H}_5\text{CH}_2\text{PO}_3\text{H}_2$: NMR (DMSO): ^1H : δ 2.97 (2H, d, $^2J_{\text{PH}}=21.5$ Hz), 7.26 (5H, m); ^{13}C { ^1H }: δ 36.20 (d, $^1J_{\text{PC}}=132.2$ Hz), 126.78 (d, $^5J_{\text{PC}}=3.4$ Hz), 128.86 (d, $^4J_{\text{PC}}=2.8$ Hz), 130.61 (d, $^3J_{\text{PC}}=6.3$ Hz), 135.03 (d, $^2J_{\text{PC}}=8.8$ Hz); ^{31}P { ^1H }: δ 22.7. ^{31}P NMR MAS: δ 31.6. IR (wavenumber/ cm^{-1}): 2757, 2309 (PO–H), 1262 (P=O), 943 (P–OH).

$4\text{-BrC}_6\text{H}_4\text{CH}_2\text{PO}_3\text{H}_2$: NMR (DMSO): ^1H : δ 2.96 (2H, d, $^2J_{\text{PH}}=21.4$ Hz), 7.21 (2H, m, *m*), 7.48 (2H, m, *o*); ^{13}C { ^1H }: δ 35.57 (d, $^1J_{\text{PC}}=131.7$ Hz), 120.00 (d, $^5J_{\text{PC}}=4.3$ Hz), 131.71 (d, $^4J_{\text{PC}}=2.8$ Hz), 132.77 (d, $^3J_{\text{PC}}=6.2$ Hz), 134.68 (d, $^2J_{\text{PC}}=8.8$ Hz); ^{31}P { ^1H }: δ 22.2. ^{31}P NMR MAS: δ 27.2. IR (wavenumber/ cm^{-1}): 2707, 2257 (PO–H), 1260 (P=O), 946 (P–OH).

$\text{Al}(\text{OH})(\text{O}_3\text{PCH}_2\text{C}_6\text{H}_4\text{Br})\cdot\text{H}_2\text{O}$ [**1a**] was prepared from 0.669 g of aluminium nitrate nonahydrate (1.78 mmol) and 1.796 g of 4-bromobenzylphosphonic acid (7.16 mmol) dissolved in 20 ml of water (1.1 mol) (Al/P/H₂O: 1/4/623). A white suspension was obtained with an initial pH of 1.50; the suspension was stirred for 30 min and then introduced in a 73 ml glass tube which was sealed and placed at 180 °C for 4 days. The resulting white powder was isolated from a yellow liquid by filtration, washed with 50 ml of water and 50 ml of ethanol, and dried at room temperature for 12 hours (0.493 g, yield 89%). (Elemental analysis found (calc.): Al 8.62 (8.68), P 10.25 (9.96), C 27.14 (27.03), H 2.95 (2.92), Br 24.94 (25.69)%.)

$\text{Al}(\text{OH})(\text{O}_3\text{PCH}_2\text{C}_6\text{H}_5)\cdot\text{H}_2\text{O}$ [**2a**] was prepared from 0.312 g of aluminium sulfate octadecahydrate (0.47 mmol) and 0.644 g of benzylphosphonic acid (3.74 mmol) dissolved in 27 ml of water (1.5 mol) (Al/P/H₂O: 1/4/1602). After 30 min stirring, the solution, for which the initial pH was 1.50, was introduced in a 98 ml glass tube which was sealed and placed at 180 °C for 6 days. The resulting white powder was isolated from a colorless liquid by filtration, washed with 50 ml of water and 50 ml of ethanol, and dried at room temperature for 12 hours (0.186 g, yield 86%). (Elemental analysis found (calc.): Al 11.44 (11.62), P 13.94 (13.34), C 36.37 (36.22), H 4.30 (4.34)%.)

$\text{Al}_2(\text{O}_3\text{PC}_6\text{H}_5)_3\cdot\text{H}_2\text{O}$ [**3a**] was prepared from 0.940 g of aluminium nitrate nonahydrate (2.5 mmol) and 1.581 g of phenylphosphonic acid (10 mmol) dissolved in 27 ml of water (1.5 mol) (Al/P/H₂O: 1/4/600). The mixture, with an initial pH of 0.85, was stirred for 30 min and then introduced into a 98 ml glass tube and subsequently sealed. The tube was stored at 180 °C for 14 days and thoroughly shaken at daily intervals.

The resulting white powder was separated from a yellow liquid by filtration, washed successively with 50 ml of water and 50 ml of acetone, and dried at room temperature for 12 hours (0.642 g, yield 95%). (Elemental analysis found (calc.): Al 10.05 (9.99), P 17.05 (17.20), C 39.99 (40.02), H 3.24 (3.17)%.)

Instrumentation

FTIR spectra were carried out on a Perkin-Elmer 1600 spectrometer under air using KBr pellets. ^1H NMR (200 MHz), ^{13}C NMR (50.28 MHz) and ^{31}P NMR (81.01 MHz) spectra were recorded on a Bruker AVANCE DPX 200 spectrometer and internally referenced to tetramethylsilane (^1H and ^{13}C) and 85% phosphoric acid (^{31}P). ^{27}Al MAS NMR spectra were recorded on a Bruker AMX-400 spectrometer, with a 4 mm rotor, at 104.26 MHz, spinning rate 12 kHz, and referenced to a 1.5 M aqueous solution of aluminium chloride hexahydrate. All isotropic chemical shifts for aluminium nuclei were obtained *via* a fit of the signal using the Bruker Win-Fit software. ^{31}P MAS NMR spectra were recorded on a Bruker DPX-300 spectrometer, with a 4 mm rotor, at 121.50 MHz with proton decoupling, spinning rate 10 kHz, and referenced to a 30% aqueous solution of H_3PO_4 . The spectra were recorded at several spinning speeds in order to identify the spinning side bands. Thermogravimetric analyses were carried out on a NETZSCH 409 thermobalance, under flowing air, at 5 °C min^{-1} ; dehydration temperatures were determined from the minima of the derivative curves of TGA graphs.

Crystallographic study

Room temperature X-ray powder diffraction patterns were recorded in the Debye–Scherrer geometry using an INEL diffractometer equipped with a CPS 120 detector, with Cu-K α_1 radiation (40 kV \times 30 mA). Samples were sieved (<63 nm) and placed in 0.3 mm diameter capillaries. Peak positions were determined using the WinPLOTR package (β version/LLB march 99); these positions were then processed by the auto-indexing program DICVOL91.²² Particularly, the powder pattern of $\text{Al}(\text{OH})(\text{O}_3\text{PCH}_2\text{C}_6\text{H}_4\text{Br})\cdot\text{H}_2\text{O}$ appeared to be suitable for a further crystallographic study. Auto-indexing of its PXRD pattern gave the initial cell parameters ($a=16.50$ Å, $b=7.06$ Å, $c=9.49$ Å, $\beta=113.47^\circ$, figure of merit $M(23)=38^{23}$). From the systematic absences, the space group $P2_1/c$ appeared likely. The FULLPROF program²⁴ was used on pattern matching mode to refine cell and peak shape parameters. In order to extract the intensities of the individual reflections, the EXTRA package²⁵ was used (Le Bail algorithm²⁶ combined with least-squares cycles to calculate optimised integrated intensities). The file of reflections generated was then input to the direct-method package SIRPOW92.²⁷ From the solution proposed, a Rietveld refinement²⁸ was carried out with FULLPROF. Atomic positions were initially refined with fixed thermal parameters. Then thermal parameters alone were refined; a refinement of thermal parameters and occupancy factors together confirmed the values of the thermal parameters as they did not shift and as occupancy factors stayed at 1.0. A final refinement of atomic coordinates along with thermal parameters was carried out. Crystallographic data are given in Table 1 and the final Rietveld difference plot is shown in Fig. 2. Atomic and isotropic thermal parameters are listed in Table 2 and selected bond lengths and angles in Table 3. The powder thermogravimetry study was carried out in the Bragg–Brentano geometry using a Philips PW1050 diffractometer (horizontal axis, Cu-K α_1 + K α_2 radiation 40 kV \times 20 mA) equipped with an Anton Paar HTK16 chamber. Samples were deposited on the upper side of a platinum foil, the temperature probe being underneath it. Patterns were collected 15 min after the given

Table 1 Crystallographic data and refinement parameters for Al(OH)(O₃PCH₂C₆H₄Br)·H₂O

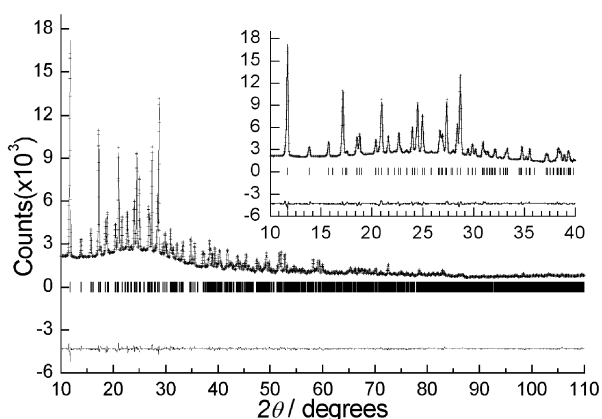
Compound	Al(OH)(O ₃ PCH ₂ C ₆ H ₄ Br)·H ₂ O
<i>M</i> /g mol ⁻¹	311.01
Crystal system	Monoclinic
Space group	<i>P</i> 2 ₁ / <i>c</i> (no. 14)
<i>a</i> /Å	16.4972(2)
<i>b</i> /Å	7.0673(1)
<i>c</i> /Å	9.4950(2)
β /°	113.477(1)
<i>V</i> /Å ³	1015.39(6)
<i>T</i> /K	298
λ (Cu-K α_1)	1.5406
<i>Z</i>	4
<i>D_c</i> /g cm ⁻³	2.034
2θ range/°	10–110
No. of reflections	1279 (357 independent)
No. of structural parameters	50
No. of profile parameters	11
$R_p = \sum y_{\text{obs}} - y_{\text{calc}} / \sum y_{\text{obs}}$	9.87
$R_{\text{wp}} = [\sum w_i y_{\text{obs}} - y_{\text{calc}} ^2 / \sum w_i (y_{\text{obs}})^2]^{1/2}$	9.21
$R_B = \sum I k_{\text{obs}} - I k_{\text{calc}} / \sum I k_{\text{obs}}$	5.79
GOF = ($R_{\text{wp}}/R_{\text{exp}}$) ²	1.26

temperature was reached, between 4 and 40° 2θ with a step size of 0.04° 2θ and a counting time of 1 s per step.

Results

Al(OH)(O₃PCH₂C₆H₄Br)·H₂O **1a**

The structure of this aluminium bromobenzylphosphonate consists of layers of both corner-sharing AlO₆ octahedra and PO₃C tetrahedra. Bromobenzyl groups extend out from both sides of the layer (Figs. 3a and 3b). The sp³ carbon (labeled C(2)) connects the phosphorus atom to the phenyl ring on C(3). The P–C(2) bond makes angles of 87.3(6)° and 103.4(6)° with respect to *b* and *c* respectively (Table 3), and the P–C(2)–C(3) angle is equal to 107(1)°: this results in a tilting of the phenyl ring with respect to the perpendicular of the layer. Within each layer, corner-sharing AlO₆ octahedra form chains running parallel to the *b* axis (Fig. 4), cross-linked by phosphonate tetrahedra. These chains are made up of aluminium and hydroxo oxygens O(5). Coordinated water appeared as the oxygen labelled O(2). Each phosphonate oxygen atom is bonded to only one aluminium atom (phosphorus connectivity (111)). The O(3) and O(4) phosphonate oxygen atoms are linked to two aluminium atoms from the same chain; the third phosphonate oxygen atom O(1) forms the bridge to a neighboring chain. The structure of the layers is very similar to the structure of the layers in ζ -Al(OH)(O₃PCH₃)·H₂O^{15,16} even though some distortions appear which could be attributed to steric constraints brought about by the bromobenzyl group. On the Al–(OH)–Al chain, two Al–O(5) distances at 1.87(2) Å

**Fig. 2** Rietveld refinement plot for Al(OH)(O₃PCH₂C₆H₄Br)·H₂O **1a**.**Table 2** Fractional atomic coordinates and equivalent isotropic displacement parameters for Al(OH)(O₃PCH₂C₆H₄Br)·H₂O

Atom	Site	<i>x</i>	<i>y</i>	<i>z</i>	<i>B_{eq}</i> ^a /Å ²
Br	4e	0.4478(2)	−0.3555(4)	0.8216(2)	4.32(5)
P	4e	0.1173(3)	0.3668(8)	0.5412(5)	1.2(1)
Al	4e	0.0047(3)	0.122(1)	0.2461(6)	1.0(1)
O(1)	4e	0.1022(4)	0.359(2)	0.6897(9)	0.62(9)
O(2)	4e	−0.0965(5)	0.103(2)	0.3218(9)	0.62
O(3)	4e	0.0766(6)	0.547(1)	0.453(1)	0.62
O(4)	4e	0.0797(6)	0.185(1)	0.452(1)	0.62
O(5)	4e	−0.0380(4)	0.373(2)	0.1892(8)	0.62
C(1)	4e	0.3710(8)	−0.123(2)	0.755(2)	0.3(1)
C(2)	4e	0.2355(8)	0.379(2)	0.578(1)	0.3
C(3)	4e	0.2742(8)	0.192(2)	0.640(2)	0.3
C(4)	4e	0.3316(9)	0.179(2)	0.796(2)	0.3
C(5)	4e	0.3199(8)	−0.138(2)	0.594(1)	0.3
C(6)	4e	0.3850(8)	0.017(2)	0.865(2)	0.3
C(7)	4e	0.2653(8)	0.036(2)	0.537(1)	0.3

$${}^a B_{\text{eq}} = 8\pi^2 \times U_{\text{eq}}$$

and 1.91(2) Å have been found, besides a unique distance at 1.87 Å for ζ -Al(OH)(O₃PCH₃)·H₂O. Aluminium–phosphonate oxygen distances in the bromobenzyl compound are 0.03 Å higher than for the methyl analog as could be expected for higher steric constraints. Alternatively, the Al–O(2) distance, where O(2) denotes the coordinated water, is equal to the distance obtained for the methylphosphonate: this result may be due to the fact that this oxygen atom is not involved directly on the constraints field as are the phosphonate oxygen atoms. The same type of structure for the inorganic layers has also been reported for Ga(OH)(O₃PC₂H₄CO₂H)·H₂O⁸ with a Ga–(OH)–Ga chain and for (VO)(O₃PC₆H₅)·H₂O²⁹ with a V=O–V chain.

The IR spectrum of Al(OH)(O₃PCH₂C₆H₄Br)·H₂O (Fig. 5) showed two broad bands at 3500 and 3382 cm⁻¹ (νOH), a sharp one at 3654 cm⁻¹ (νOH) and a relatively thin band at 1646 cm⁻¹ (δOH). The two broad bands typical of water-containing compounds may be due to the splitting of vibration modes because of the existence of two hydrogen bonds with different lengths, as seen on the single crystal structure of ζ -Al(OH)(O₃PCH₃)·H₂O; this has already been observed, for instance on copper phosphonates.^{30,31}

The ²⁷Al MAS NMR spectrum exhibited a specially broad and asymmetric signal because of the quadrupolar effect of the

Table 3 Selected bond distances (Å) and angles (°) for Al(OH)(O₃PCH₂C₆H₄Br)·H₂O

Al–O(1) ⁱ	1.89(1)	P–O(1)	1.53(1)
Al–O(2)	2.07(1)	P–O(3)	1.53(1)
Al–O(3) ⁱⁱ	1.91(1)	P–O(4)	1.52(2)
Al–O(4)	1.91(1)	P–C(2)	1.84(1)
Al–O(5)	1.91(2)	C(2)–C(3)	1.48(2)
Al–O(5) ⁱⁱ	1.87(2)	Br–C(1)	2.01(2)
O(1) ⁱ –Al–O(2)	176.4(4)	O(1)–P–O(3)	109.9(6)
O(1) ⁱ –Al–O(3) ⁱⁱ	94.6(4)	O(1)–P–O(4)	107.4(6)
O(1) ⁱ –Al–O(4)	89.7(4)	O(1)–P–C(2)	112.1(5)
O(1) ⁱ –Al–O(5)	96.5(6)	O(3)–P–O(4)	113.9(6)
O(1) ⁱ –Al–O(5) ⁱⁱ	89.3(6)	O(3)–P–C(2)	105.5(6)
O(2)–Al–O(3) ⁱⁱ	88.9(4)	O(4)–P–C(2)	108.1(6)
O(2)–Al–O(4)	86.7(4)		
O(2)–Al–O(5)	84.3(5)	P–C(2)–C(3)	106.9(10)
O(2)–Al–O(5) ⁱⁱ	89.9(5)	C(2)–P···P ^{iv}	87.3(6)
O(3) ⁱⁱ –Al–O(4)	175.0(6)	C(2)–P···P ^v	103.4(6)
O(3) ⁱⁱ –Al–O(5)	86.7(4)		
O(3) ⁱⁱ –Al–O(5) ⁱⁱ	93.6(6)	Br–C(1)–C(5)	107.9(10)
O(4)–Al–O(5)	95.1(6)	Br–C(1)–C(6)	116.7(9)
O(4)–Al–O(5) ⁱⁱ	84.1(4)		
O(5)–Al–O(5) ⁱⁱ	174.1(3)		
Al–O(5)–Al ⁱⁱⁱ	138.8(7)		

^aSymmetry codes: i = *x*, ½–*y*, *z*–½; ii = –*x*, *y*–½, ½–*z*; iii = 1–*x*, ½+*y*, ½–*z*; iv = *x*, 1+*y*, *z*; v = *x*, *y*, 1+*z*.

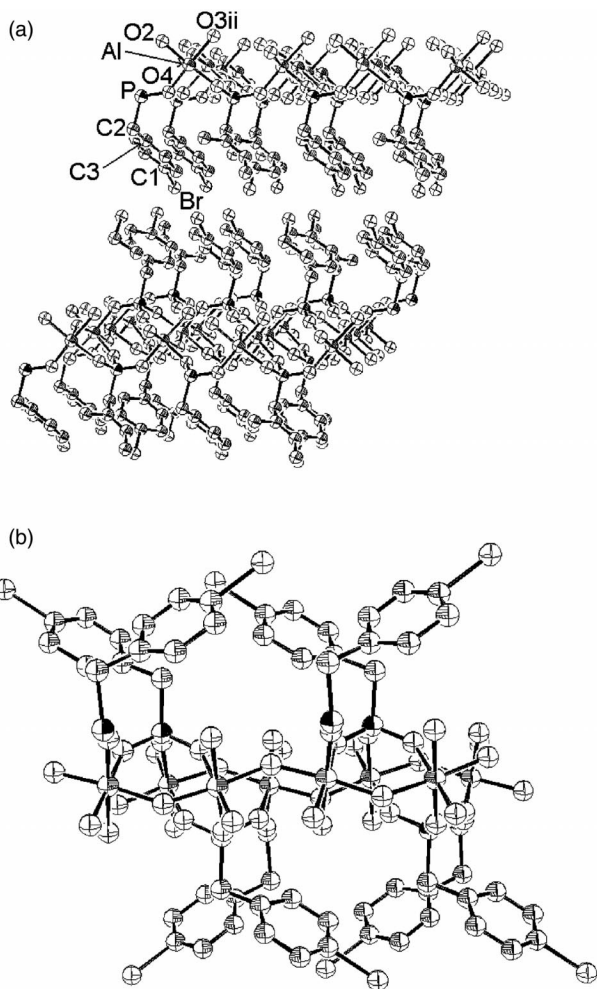


Fig. 3 Perspective view of the structure of $\text{Al(OH)(O}_3\text{PCH}_2\text{C}_6\text{H}_4\text{Br)}\cdot\text{H}_2\text{O}$ down the b axis (a) and the view down the c axis (b).

^{27}Al nucleus. From simulation of this signal, we obtained an isotropic chemical shift of 1.1 ppm attributable to an octahedral environment for the aluminium atom (Fig. 6 and Table 4). The FWHM value obtained was 2380 Hz/9.4 T. The ^{31}P MAS NMR spectrum (Fig. 7) showed only one, nevertheless relatively broad, site for the phosphorus atoms (δ 11.1).

Thermogravimetric analysis revealed a first mass loss of 5.7% (theoretical mass loss for one water molecule: 5.8%) at 215 °C (Fig. 8). The second mass loss at 332 °C corresponding to the elimination of the hydroxyl group (experimental and calculated

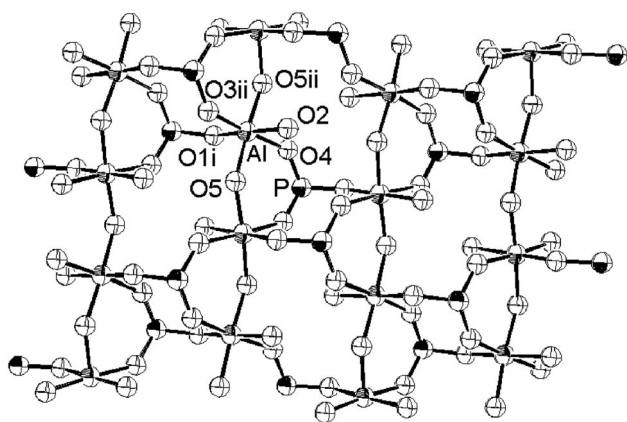


Fig. 4 View of the (bc) plane of $\text{Al(OH)(O}_3\text{PCH}_2\text{C}_6\text{H}_4\text{Br)}\cdot\text{H}_2\text{O}$. Carbon and bromine atoms have been omitted for clarity.

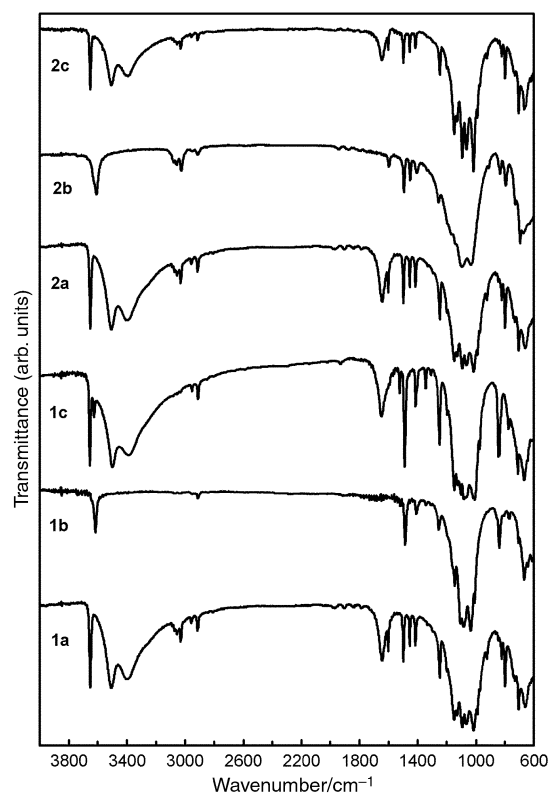


Fig. 5 IR spectra of $\text{Al(OH)(O}_3\text{PCH}_2\text{C}_6\text{H}_4\text{Br)}\cdot\text{H}_2\text{O}$ **1a**, $\text{Al(OH)(O}_3\text{PCH}_2\text{C}_6\text{H}_4\text{Br)}$ **1b** and the related compound **1c** (obtained by stirring **1b** in water for two days), $\text{Al(OH)(O}_3\text{PCH}_2\text{C}_6\text{H}_5)\cdot\text{H}_2\text{O}$ **2a**, $\text{Al(OH)(O}_3\text{PCH}_2\text{C}_6\text{H}_5)$ **2b** and the related rehydrated compound **2c**.

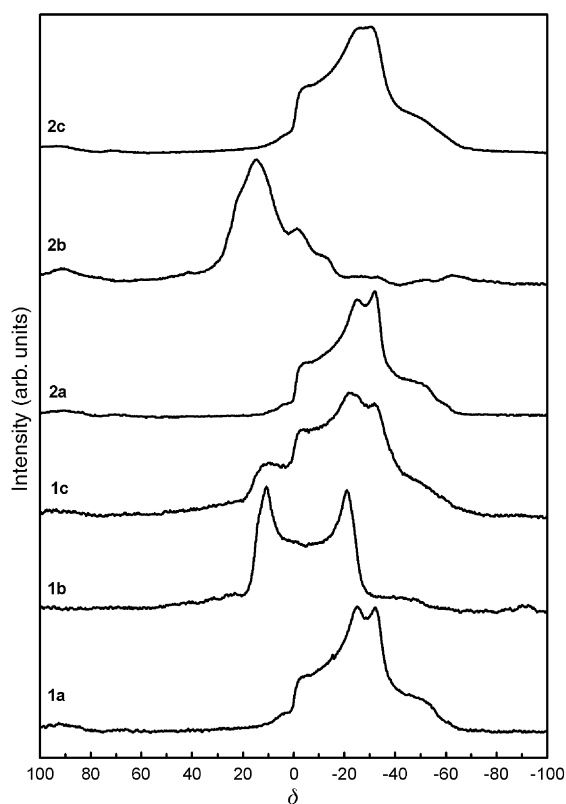


Fig. 6 ^{27}Al MAS NMR spectra of $\text{Al(OH)(O}_3\text{PCH}_2\text{C}_6\text{H}_4\text{Br)}\cdot\text{H}_2\text{O}$ **1a**, $\text{Al(OH)(O}_3\text{PCH}_2\text{C}_6\text{H}_4\text{Br)}$ **1b** and related compound **1c** (obtained by stirring **1b** in water for two days), $\text{Al(OH)(O}_3\text{PCH}_2\text{C}_6\text{H}_5)\cdot\text{H}_2\text{O}$ **2a**, $\text{Al(OH)(O}_3\text{PCH}_2\text{C}_6\text{H}_5)$ **2b** and related rehydrated compound **2c**.

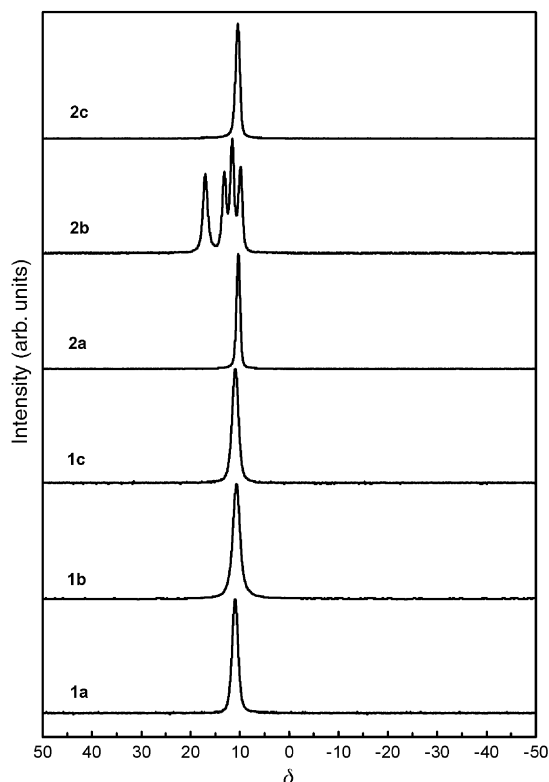


Fig. 7 ^{31}P MAS NMR spectra of $\text{Al(OH)(O}_3\text{PCH}_2\text{C}_6\text{H}_4\text{Br)}\cdot\text{H}_2\text{O}$ **1a**, $\text{Al(OH)(O}_3\text{PCH}_2\text{C}_6\text{H}_4\text{Br)}$ **1b** and related compound **1c** (obtained by stirring **1b** in water for two days), $\text{Al(OH)(O}_3\text{PCH}_2\text{C}_6\text{H}_5)\cdot\text{H}_2\text{O}$ **2a**, $\text{Al(OH)(O}_3\text{PCH}_2\text{C}_6\text{H}_5)$ **2b** and related rehydrated compound **2c**.

value: 8.7%) occurred just before the degradation of the organic groups (experimental mass loss of 58.7% for a theoretical value of 60.8%). The residual compound was identified to be AlPO_4 on the basis of PXRD.

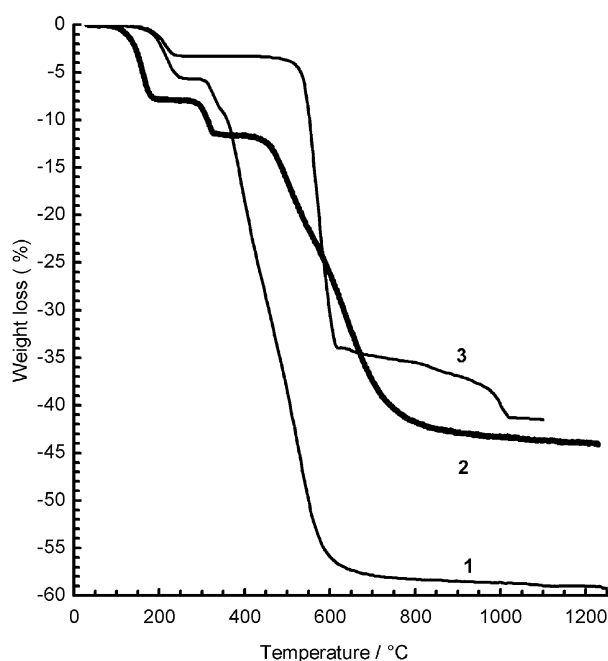
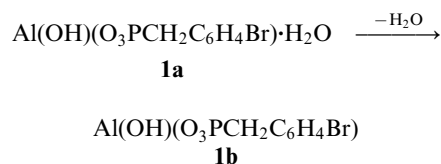


Fig. 8 TGA curves of $\text{Al(OH)(O}_3\text{PCH}_2\text{C}_6\text{H}_4\text{Br)}\cdot\text{H}_2\text{O}$ **1**, $\text{Al(OH)(O}_3\text{PCH}_2\text{C}_6\text{H}_5)\cdot\text{H}_2\text{O}$ **2** and $\text{Al}_2(\text{O}_3\text{PC}_6\text{H}_5)_3\cdot\text{H}_2\text{O}$ **3**.

Table 4 ^{27}Al NMR parameters for $\text{Al(OH)(O}_3\text{PCH}_2\text{C}_6\text{H}_4\text{Br)}\cdot\text{H}_2\text{O}$ **1a** and its related compound **1b**, $\text{Al(OH)(O}_3\text{PCH}_2\text{C}_6\text{H}_5)\cdot\text{H}_2\text{O}$ **2a**, its related compound **2c**, $\text{Al}_2(\text{O}_3\text{PC}_6\text{H}_5)_3\cdot\text{H}_2\text{O}$ **3a** (two sites), its related compound **3c** (two sites)

	δ_{iso}^a	C_Q^b / kHz	η_Q^c
1a	1.1	6520	0.74
1b	24.2	7380	0.11
2a	0.5	6420	0.74
2c	1.6	6480	0.75
3a	51.4 -13.4	4530 4430	0.50 0.56
3c	50.6 -13.5	4450 4530	0.48 0.57

^aIsotropic chemical shift. ^bQuadrupolar coupling constant. ^cAsymmetry factor.



An IR spectrum of the bromobenzyl dehydrated compound **1b** obtained at 280 °C (Fig. 5) showed the disappearance of the bands at 1646, 3500 and 3382 cm^{-1} . The band at 3617 cm^{-1} for **1b** seems to result from the shift of the band seen at 3654 cm^{-1} for **1a**. Although strong modifications in the PO_3 vibration region appeared in the IR spectrum, the ^{31}P NMR signal (Fig. 7) did not shift (δ 11.0): thus it seems that the (111) connectivity of the phosphonate oxygens does not change upon dehydration.³² The ^{27}Al NMR spectrum for the dehydrated bromobenzylphosphonate (Fig. 6) showed a single signal exhibiting a new shape, with an isotropic chemical shift of 24.2 ppm and a small asymmetry factor (Table 4). This chemical shift may be attributed to the formation of 5-coordinate aluminium due to the release of the coordinated water. From the IR spectrum obtained for the dehydrated compound **1b** stirred in water at ambient temperature for two days (resulting sample **1c**), one could suppose that the rehydration was completed (Fig. 5). However, the ^{27}Al NMR spectrum of the previous sample **1c** showed the superimposi-

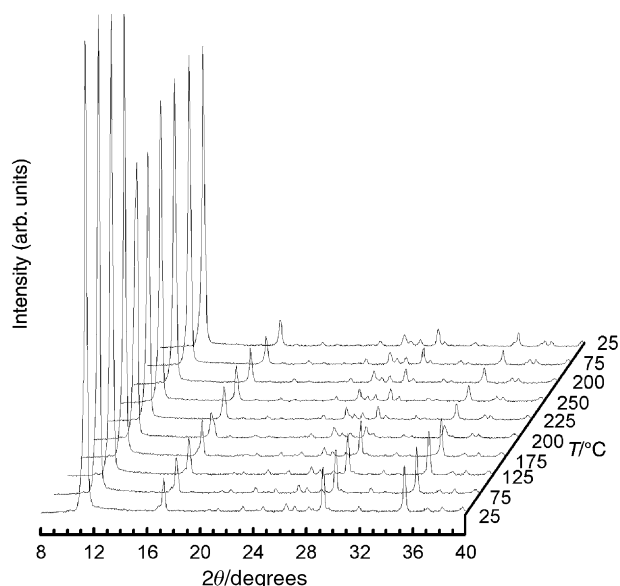


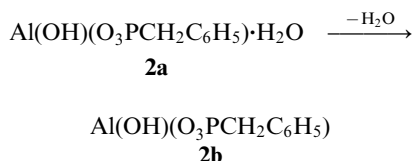
Fig. 9 Thermodiffractogram of compound **1** (initially $\text{Al(OH)(O}_3\text{PCH}_2\text{C}_6\text{H}_4\text{Br)}\cdot\text{H}_2\text{O}$).

tion of the signals from **1a** and **1b** implying that the rehydration reaction was not fully completed. The thermodiffraction study presented in Fig. 9 showed the phase transition to occur at around 200 °C, clearly related to the dehydration. No modification of the interlamellar distance was noticeable. On cooling, the diffractogram presented at 25 °C was recorded after 1 hour at this temperature, which did not allow us to observe the features of the initial compound.

Al(OH)(O₃PCH₂C₆H₅)·H₂O **2a**

Automatic powder indexation of the benzylphosphonate **2a** (Fig. 10) was carried out with 15 peaks and yielded a monoclinic system ($a=14.96$ Å, $b=7.06$ Å, $c=9.52$ Å, $\beta=114.30^\circ$, $M(15)=14^{23}$). The b and c parameters are very close to those describing the inorganic layers of Al(OH)(O₃PCH₂C₆H₄Br)·H₂O and ζ -Al(OH)(O₃PCH₃)·H₂O. The IR spectrum (Fig. 5) showed two broad bands at 3508 and 3396 cm⁻¹, the sharp band at 3651 cm⁻¹, the band at 1643 cm⁻¹ and a PO₃ region highly similar to the PO₃ region for **1a**. The isotropic chemical shift of the broad and asymmetric ²⁷Al MAS NMR signal was found at 0.5 ppm (Fig. 6 and Table 4) and the ³¹P MAS NMR signal at 10.4 ppm (Fig. 7).

Thermogravimetric analysis showed a first mass loss of 7.5% at 147 °C (Fig. 8), which corresponded to the release of one water molecule (theoretical mass loss: 7.8%). The second mass loss at 307 °C corresponded to the elimination of the hydroxyl group and gave a total mass loss (water+hydroxyl group) of 11.4% for an expected value of 11.6%. Weight losses above 380 °C were due to the degradation of the organic groups, with formation of AlPO₄ (observed mass loss of 45.2% for an expected value of 47.5%).



The IR spectrum of the dehydrated compound **2b** obtained at 230 °C (Fig. 5) was similar to the spectrum of **1b**. On the ²⁷Al NMR spectrum (Fig. 6) we observed a new signal with its maximum at 14.5 ppm. Attempts to simulate this signal did not lead to a single site nor to sites with reasonable quadrupolar coupling constants, but always to isotropic chemical shifts which might correspond to Al–O₅ coordination. Surprisingly, we observed four bands on the ³¹P NMR spectra of **2b** (Fig. 7). Nevertheless, when this dehydrated compound **2b** was exposed to ambient moisture for 6 hours it resulted in the sample **2c** which was identical to the initial compound, as can be seen in the IR and NMR spectra (Figs. 5, 6 and 7 and Table 4) thus showing the spontaneous rehydration. The thermodiffraction (Fig. 11) exhibits an unexpected increase in the interlamellar distance around 150 °C (+0.6 Å) which may be attributed to a slight displacement of the benzyl groups toward a less well-packed arrangement. On cooling, the pattern obtained after 3 h at 25 °C shows features of the initial compound, confirming the reversibility of the dehydration reaction.

Al₂(O₃PC₆H₅)₃·H₂O **3a**

The formation of benzyl derivatives **1a** and **2a** under hydrothermal conditions (in a sealed glass tube at 180 °C—see Experimental section) was found to be independent from the Al/P molar ratio for reactants in the initial solution (from 0.25 to 1). In contrast this ratio was found to be one of the determining parameters for the synthesis of the phenyl derivatives. The reaction of equimolar amounts of aluminium nitrate and phenylphosphonic acid led to Al(OH)(O₃PC₆H₅)

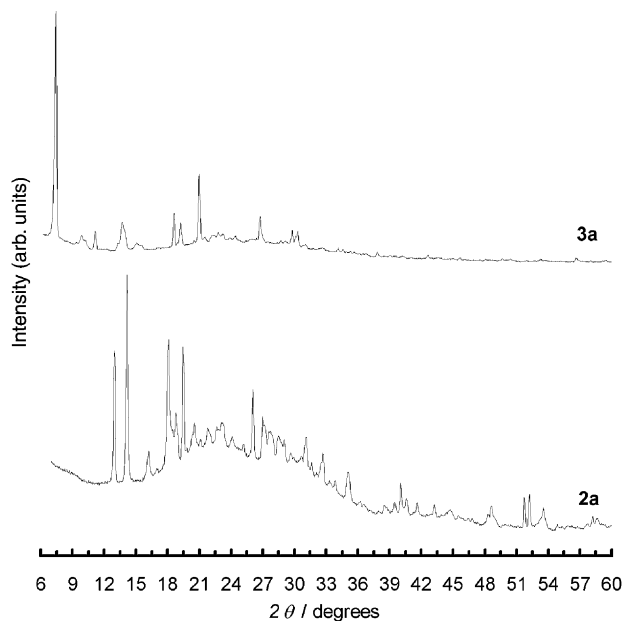


Fig. 10 Powder X-ray diffraction patterns of Al(OH)(O₃PCH₂C₆H₅)·H₂O **2a** and Al₂(O₃PC₆H₅)₃·H₂O **3a**.

which was previously obtained by Cabeza *et al.* by another route.¹⁹ The reaction of aluminium nitrate and phenylphosphonic acid with a Al/P molar ratio of 1/4 led after 5 days to α -Al(HO₃PC₆H₅)(O₃PC₆H₅)·H₂O, which was also previously obtained by Cabeza *et al.* by reaction of aluminium chloride and phenylphosphonic acid. However, shaking and 14 days synthesis time led to the synthesis of a *novel phase*, as shown by XRD, even if the compounds were poorly crystalline (Fig. 10). This result is evidence that α -Al(HO₃PC₆H₅)(O₃PC₆H₅)·H₂O is a kinetically favoured intermediate phase. This last compound was found to be lamellar.¹⁹ As to the novel phase (hereafter labelled **3a**), 15 peaks were extracted from the powder pattern and subsequently processed using an auto-indexing program. Even though the suggested cell parameters (monoclinic system, $a=26.77$ Å, $b=9.28$ Å, $c=9.57$ Å, $\beta=117.34^\circ$) are given with a moderate reliability ($M(15)\approx 12^{23}$), the stacking parameter

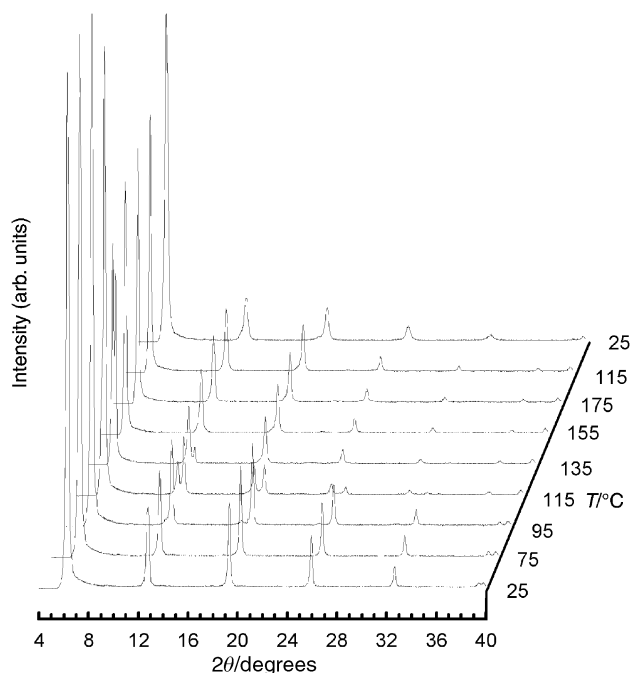


Fig. 11 Thermodiffraction of compound **2** (initially Al(OH)(O₃PCH₂C₆H₅)·H₂O).

Table 4) and subsequent TGA. The thermodiffractogram exhibits clearly the phase transition around 175 °C as well as the reversibility of the dehydration reaction (Fig. 15). During the dehydration, the stacking parameter drops down to 23.14 Å.

Moreover attempts to obtain $\text{Al}_2(\text{O}_3\text{PC}_6\text{H}_5)_3 \cdot 2\text{H}_2\text{O}$ by hydration of $\text{Al}_2(\text{O}_3\text{PC}_6\text{H}_5)_3 \cdot \text{H}_2\text{O}$ by stirring it at ambient temperature in water for three days did not succeed, thus showing the stability of the monohydrated phase under these conditions.

Discussion

Synthesis

The versatility of the synthesis of aluminium phenylphosphonates has been previously highlighted.^{19,33,34} The formation of $\text{Al}(\text{HO}_3\text{PC}_6\text{H}_5)(\text{O}_3\text{PC}_6\text{H}_5) \cdot \text{H}_2\text{O}$ was reported from an aqueous solution of aluminium nitrate and phenylphosphonic acid with a Al/P ratio of 0.25, using refluxing conditions instead of hydrothermal conditions.³³ The literature also gives some indications about the influence of the aluminium precursor: AlCl_3 and $\text{Al}_2(\text{SO}_4)_3$,¹⁹ or bayerite.³⁴ Although a complete discussion of synthesis parameters (role of pH, temperature, pressure *etc.*) is beyond the scope of this article, two aspects are worth pointing out from the present work. First, the Al/P ratio in the initial mixture seems to be the key factor that directs the synthesis toward $\text{Al}_2(\text{O}_3\text{PC}_6\text{H}_5)_3 \cdot \text{H}_2\text{O}$ [3a] (Al/P = 0.25) or $\text{Al}(\text{OH})(\text{O}_3\text{PC}_6\text{H}_5)$ (Al/P = 1). Moreover, we herein show that shaking and a longer heating time yields $\text{Al}_2(\text{O}_3\text{PC}_6\text{H}_5)_3 \cdot \text{H}_2\text{O}$ [3a] rather than $\alpha\text{-Al}(\text{HO}_3\text{PC}_6\text{H}_5)(\text{O}_3\text{PC}_6\text{H}_5) \cdot \text{H}_2\text{O}$ obtained with a shorter heating time. Thus, the straightforward formation of a kinetically-favoured compound such as $\alpha\text{-Al}(\text{HO}_3\text{PC}_6\text{H}_5)(\text{O}_3\text{PC}_6\text{H}_5) \cdot \text{H}_2\text{O}$ may hide the existence of a second compound such as $\text{Al}_2(\text{O}_3\text{PC}_6\text{H}_5)_3 \cdot \text{H}_2\text{O}$ [3a].

Structural characterisation

The difference observed between the structure of $\text{Al}(\text{OH})(\text{O}_3\text{PCH}_2\text{C}_6\text{H}_4\text{Br}) \cdot \text{H}_2\text{O}$ [1a] and $\text{Al}(\text{OH})(\text{O}_3\text{PCH}_2\text{C}_6\text{H}_5) \cdot \text{H}_2\text{O}$ [2a] on the one hand, and the structure of $\text{Al}(\text{OH})(\text{O}_3\text{PC}_6\text{H}_5)$ ¹⁹ on the other, is noteworthy. The similarities of the structures of the benzyl derivatives with the methyl analog $\zeta\text{-Al}(\text{OH})(\text{O}_3\text{PCH}_3) \cdot \text{H}_2\text{O}$ ^{15,16} may be related to

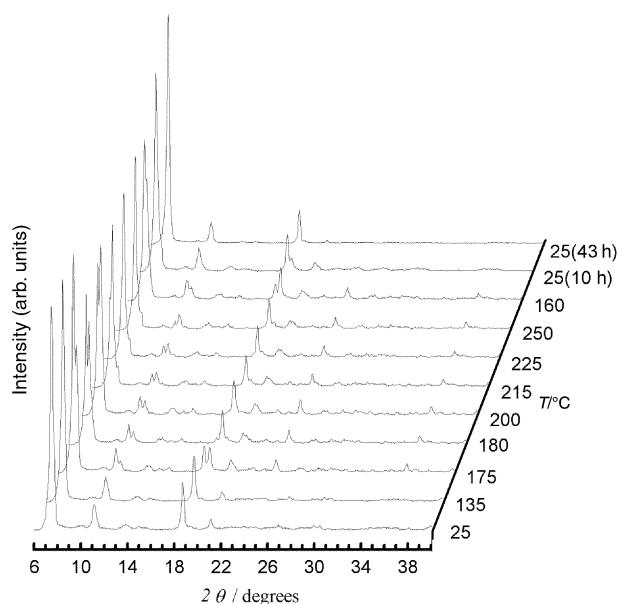


Fig. 15 Thermodiffractogram of compound 3 (initially $\text{Al}_2(\text{O}_3\text{PC}_6\text{H}_5)_3 \cdot \text{H}_2\text{O}$).

the benzyl flexibility, that allows a high packing within the layers similar to the methyl phase. Such a flexibility does not exist in the phenyl phase because of the direct phosphorus–phenyl bond.

Based on the formula, the suggested cell parameters and the IR and NMR spectra, it is clear that $\text{Al}_2(\text{O}_3\text{PC}_6\text{H}_5)_3 \cdot \text{H}_2\text{O}$ [3a] is structurally different from $\text{Al}_2(\text{O}_3\text{PC}_6\text{H}_5)_3 \cdot 2\text{H}_2\text{O}$;¹⁹ this structural difference gives an explanation for our failure to convert 3a into $\text{Al}_2(\text{O}_3\text{PC}_6\text{H}_5)_3 \cdot 2\text{H}_2\text{O}$ by hydration. Despite the poverty of the PXRD data we can infer some structural information about 3a: if we assume that the PO_3 groups are in (111) connectivity, we have 9 oxygen atoms per formula to which we add the one from the water. The resulting count is consistent with the ²⁷Al NMR spectrum (Fig. 13) as it implies 4 oxygen atoms for the tetrahedral environment of aluminium atoms and 6 for the octahedral environment. The water should thus belong to the octahedral coordination since its signal is the most perturbed upon dehydration.

Dehydration–hydration reactions

A common feature for monohydrated phases 1a, 2a and 3a is that the water molecule is bonded to the aluminium atom, that dehydration takes place around 150–200 °C and is reversible, even though the rehydration rate is much lower for 1a (probably due to steric hindrance).

It is noteworthy that despite the high structural similarity between 1a and 2a, ²⁷Al NMR spectra indicate different environments around the aluminium atoms for the dehydrated compounds 1b and 2b, and ³¹P MAS NMR spectra show a single site for 1b but four sites for 2b. Also, this dehydration occurs without noticeable modification of the interlamellar distance for the bromobenzyl derivative while a small increase in the interlamellar distance was observed for the benzyl derivative.

The dehydration of 3a took place near 200 °C, whereas $\text{Al}_2(\text{O}_3\text{PC}_6\text{H}_5)_3 \cdot 2\text{H}_2\text{O}$ was reported to undergo a one-step dehydration reaction as early as 60 °C,¹⁹ thus illustrating the influence of the structure on the dehydration behaviour. It is difficult to compare unambiguously the dehydrated compound 3b with the compound obtained by Cabeza *et al.* from the dehydration of $\text{Al}_2(\text{O}_3\text{PC}_6\text{H}_5)_3 \cdot 2\text{H}_2\text{O}$, because of the lack of information on the PRXD patterns. However 3b easily rehydrated over a few minutes into the initial monohydrated compound 3a, whereas the dehydrated compound arising from $\text{Al}_2(\text{O}_3\text{PC}_6\text{H}_5)_3 \cdot 2\text{H}_2\text{O}$ hardly rehydrated over several days. These observations suggest that the dehydration reactions of $\text{Al}_2(\text{O}_3\text{PC}_6\text{H}_5)_3 \cdot 2\text{H}_2\text{O}$ and 3a lead to two different compounds of the same formula $\text{Al}_2(\text{O}_3\text{PC}_6\text{H}_5)_3$.

Conclusion

This work confirms the rich diversity of aluminium phosphonates. Particularly minor changes in the syntheses of aluminium phenylphosphonates lead to different stoichiometries and structures. We have shown that the study of the ternary diagram of Fig. 1 illustrates the existence of kinetic phases such as $\alpha\text{-Al}(\text{HO}_3\text{PC}_6\text{H}_5)(\text{O}_3\text{PC}_6\text{H}_5) \cdot \text{H}_2\text{O}$. Moreover the hydration–dehydration behaviour of phases closely depends on their structure. Thus, the new compound $\text{Al}_2(\text{O}_3\text{PC}_6\text{H}_5)_3 \cdot \text{H}_2\text{O}$ [3a], whose dehydration was shown to be easily reversible, could not be hydrated into $\text{Al}_2(\text{O}_3\text{PC}_6\text{H}_5)_3 \cdot 2\text{H}_2\text{O}$, whose dehydration was not observed after a few days.¹⁹

The two new benzyl phosphonates $\text{Al}(\text{OH})(\text{O}_3\text{PCH}_2\text{C}_6\text{H}_4\text{Br}) \cdot \text{H}_2\text{O}$ [1a] and $\text{Al}(\text{OH})(\text{O}_3\text{PCH}_2\text{C}_6\text{H}_5) \cdot \text{H}_2\text{O}$ [2a] also underwent reversible dehydration processes. They represent an interesting case of isostructurality with $\zeta\text{-Al}(\text{OH})(\text{O}_3\text{PCH}_3) \cdot \text{H}_2\text{O}$ as opposed to the $\text{Al}(\text{OH})(\text{O}_3\text{PC}_6\text{H}_5)$ case.

Acknowledgements

We gratefully acknowledge Catherine Deudon and the Institut des Matériaux Jean Rouxel for recording the room-temperature X-ray data.

References

- 1 A. Clearfield, *Progress in Inorganic Chemistry*, vol. 47, ed. K. D. Karlin, John Wiley & Sons Inc., , 1998.
- 2 B. Bujoli, P. Palvadeau and J. Rouxel, *Chem. Mater.*, 1990, **2**, 582.
- 3 P. Janvier, S. Drumel, Y. Piffard and B. Bujoli, *C. R. Acad. Sci. Paris*, 1995, **t. 320, Serie II**, 29.
- 4 R. C. Wang, Y. Zhang, H. Hu, R. R. Frausto and A. Clearfield, *Chem. Mater.*, 1992, **4**, 864.
- 5 G. Cao, V. M. Lynch, S. Swinnea and T. E. Mallouk, *Inorg. Chem.*, 1990, **29**, 2112.
- 6 F. Serpaggi and G. Ferey, *J. Mater. Chem.*, 1998, **8**, 2737.
- 7 J. Morizzi, M. Hobday and C. Rix, *J. Mater. Chem.*, 1999, **9**, 863.
- 8 F. Fredoueil, D. Massiot, D. Poojary, M. Bujoli-Doeuff, A. Clearfield and B. Bujoli, *Chem. Commun.*, 1998, 175.
- 9 Y. Yang, M. G. Walawalkar, J. Pinkas, H. W. Roesky and H. G. Schmidt, *Angew. Chem., Int. Ed.*, 1998, **37**, 96.
- 10 S. Oliver, A. Kuperman and G. A. Ozin, *Angew. Chem., Int. Ed.*, 1998, **37**, 45.
- 11 S. T. Wilson, B. M. Lok, C. A. Messina, T. R. Cannan and E. M. Flanigen, *J. Am. Chem. Soc.*, 1982, **104**, 1146.
- 12 M. G. Walawalkar, H. W. Roesky and R. Murugavel, *Acc. Chem. Res.*, 1999, **32**, 117.
- 13 K. Maeda, J. Akimoto, Y. Kiyozumi and F. Mizukami, *J. Chem. Soc., Chem. Commun.*, 1995, 1033.
- 14 K. Maeda, J. Akimoto, Y. Kiyozumi and F. Mizukami, *Angew. Chem., Int. Ed. Engl.*, 1995, **34**, 1199.
- 15 L.-J. Sawers, V. J. Carter, A. R. Armstrong, P. G. Bruce, P. A. Wright and B. E. Gore, *J. Chem. Soc., Dalton Trans.*, 1996, 3159.
- 16 K. Maeda, Y. Hashiguchi, Y. Kiyozumi and F. Mizukami, *Bull. Chem. Soc. Jpn.*, 1997, **70**, 345.
- 17 G. B. Hix, V. J. Carter, D. S. Wragg, R. E. Morris and P. A. Wright, *J. Mater. Chem.*, 1999, **9**, 179.
- 18 G. B. Hix, D. S. Wragg, P. A. Wright and R. E. Morris, *J. Chem. Soc., Dalton Trans.*, 1998, 3359.
- 19 A. Cabeza, M. A. G. Aranda, S. Bruque, D. M. Poojary, A. Clearfield and J. Sanz, *Inorg. Chem.*, 1998, **37**, 4168.
- 20 C. E. McKenna, M. T. Higa, N. H. Cheung and M. C. McKenna, *Tetrahedron Lett.*, 1977, 155.
- 21 A. K. Bhattacharya and G. Thygaragan, *Chem. Rev.*, 1981, **81**, 415.
- 22 A. Boultif and D. Louër, *J. Appl. Crystallogr.*, 1991, **24**, 987.
- 23 P. M. De Wolff, *J. Appl. Crystallogr.*, 1968, **5**, 108.
- 24 J. Rodriguez-Carvajal, *Collected Abstracts of Powder Diffraction Meeting*, Toulouse, France, 1990, p. 127.
- 25 A. Altomare, M. C. Burla, G. Cascarano, C. Giacovazzo, A. Guagliardi, A. G. G. Moliterni and G. Polidori, *J. Appl. Crystallogr.*, 1995, **28**, 842.
- 26 A. Le Bail, H. Duroy and J. L. Fourquet, *Mater. Res. Bull.*, 1988, **23**, 447.
- 27 A. Altomare, G. Cascarano, C. Giacovazzo, A. Guagliardi, M. C. Burla, G. Polidori and M. Camalli, *J. Appl. Crystallogr.*, 1994, **27**, 435.
- 28 H. M. Rietveld, *J. Appl. Crystallogr.*, 1969, **2**, 65.
- 29 G. Huan, A. J. Jacobson, J. W. Johnson and E. W. Corcoran, *Chem. Mater.*, 1990, **2**, 91.
- 30 Y. Zhang and A. Clearfield, *Inorg. Chem.*, 1992, **31**, 2821.
- 31 J. Le Bideau, B. Bujoli, A. Jouanneaux, C. Payen, P. Palvadeau and J. Rouxel, *Inorg. Chem.*, 1993, **32**, 4617.
- 32 D. Massiot, S. Drumel, P. Janvier, M. Bujoli-Doeuff and B. Bujoli, *Chem. Mater.*, 1997, **9**, 6.
- 33 J. E. Haky, J. B. Brady, N. Dando and D. Weaver, *Mater. Res. Bull.*, 1997, **32**, 297.
- 34 L. Raki and C. Detellier, *Chem. Commun.*, 1996, 2475.